ISSN 1063-7834, Physics of the Solid State, 2011, Vol. 53, No. 11, pp. 2290–2299. © Pleiades Publishing, Ltd., 2011.
Original Russian Text © N.G. Zamkova, V.S. Zhandun, V.I. Zinenko, 2011, published in Fizika Tverdogo Tela, 2011, Vol. 53, No. 11, pp. 2175–2184.

FERROELECTRICITY

Effect of Sr^{2+} Ion Substitution with Trivalent Ions (Sc^{3+}, In^{3+}, La^{3+}, Bi^{3+}) on Its Ferroelectric Instability in $SrTiO_3$

N. G. Zamkova, V. S. Zhandun, and V. I. Zinenko*

Kirensky Institute of Physics, Siberian Branch, Russian Academy of Science, Akademgorodok 50, Krasnoyarsk, 660036 Russia

** e-mail: zvi@iph.krasn.ru*

Received April 12, 2011

Abstract—The vibration frequencies of unstable ferroelectric and antiferrodistortion modes and the dependences of the energy on the ion displacement amplitude have been calculated within the generalized Gordon–Kim model for distortions along eigenvectors of these modes in the mixed compounds $Sr_{1-x}A_xTi_{1-x/4}\square_{x/4}O_3$ and $Sr_{1-y}A_{2y/3}\square_{y/3}TiO_3$ ($A = Sc^{3+}$, In^{3+}, La^{3+}, Bi^{3+}; $\square$ is the vacancy). To compensate an excess positive charge, vacancies are introduced into the Ti^{4+} or Sr^{2+} site. Calculations have been performed in the "average" crystal approximation for impurity concentrations of 0.25 and 0.50. To this end, a set of 40 atomic superlattices with various orderings of heterovalent ions Sr^{2+} and impurity A^{3+} has been considered. It has been found that each impurity type, independently of charge balance, induces ferroelectric instabilities in doped compounds. In the case of doping with In^{3+} and La^{3+} for concentration $x = 0.25$, the possibility of rotating the polarization vector has been shown.

DOI: 10.1134/S1063783411110345

1. INTRODUCTION

Doping of oxides with a perovskite structure by heterovalent impurities offers opportunities to develop new functional materials; a large number of experimental and theoretical works are devoted to such compounds. Introduction of heterovalent impurities into crystals with a perovskite structure changes significantly both the phase diagram and physical properties of doped compounds. For example, this takes place in manganites, where magnetic properties [1, 2] change, or in ferroelectrics with a perovskite structure, where electrical properties change [3, 4].

The $SrTiO_3$ crystal belongs to a specific class of compounds referred to as quantum paraelectrics in which, despite the anomalous behavior of permittivity, the ferroelectric state does not arise until the very low temperatures [5]. Introduction of even a small homovalent impurity content into the Sr^{2+} ion site, e.g., Ba^{2+}, results in the appearance of ferroelectricity in $Sr_{1-x}Ba_xTiO_3$ [6]. As to the question of the ferroelectricity appearance in $SrTiO_3$ doped with heterovalent impurities, it remains open. For example, in the study of $[Sr_{1-1.5x}Bi_x\square_{0.5x}]TiO_3$ [7], hysteresis loops were detected and the spontaneous polarization was estimated; at the same time, according to [8], the ferroelectric state in this compound was not detected.

Thus, the study of the effect of strontium ion substitution with trivalent ions on the lattice dynamics and ferroelectric properties is of interest. The objective of this study is to perform ab initio calculations of the vibration frequencies, permittivities, Born dynamic charges, and spontaneous polarization of the doped compounds $Sr_{1-x}A_xTi_{1-x/4}\square_{x/4}O_3$ and $Sr_{1-y}A_{2y/3}\square_{y/3}TiO_3$, where A is Sc^{3+}, In^{3+}, La^{3+}, and Bi^{3+}.

2. CALCULATION METHOD

All calculations are performed within the ab initio model of the ionic crystal, taking into account the dipole and quadrupole polarizabilities of ions [9]. To calculate the properties of the $SrTiO_3$ crystal with trivalent ion impurities, it is supposed that trivalent impurity ions occupy Sr^{2+} sites in the perovskite structure, and the ionic mechanism of charge compensation with the formation of vacancies at Ti^{4+} sites ($Sr_{1-x}A_xTi_{1-x/4}\square_{x/4}O_3$) or at Sr^{2+} sites ($Sr_{1-y}A_{2y/3}\square_{y/3}TiO_3$) is implemented. As a rule, such "mixed" compounds are calculated in the virtual crystal approximation [10]. However, in the case of a heterovalent impurity, the virtual crystal approximation can introduce a significant error into the calculation of long-range electrostatic interactions, such as the Coulomb and dipole interactions, which play an important role in the behavior of ferroelectric instabilities. In [11], to calculate structural and electronic properties of the $SrFCl_xBr_{1-x}$ alloy, a set of random configurations was used. In the present study, we used a slightly different approach to calculate the ferroelectric instability of the doped compounds $Sr_{1-x}A_x(Ti_{1-x/4}\square_{x/4})O_3$ and $(Sr_{1-y}\square_{y/3})A_{2y/3}TiO_3$: the energies of doped crystals were calculated for a set of superlattices with various

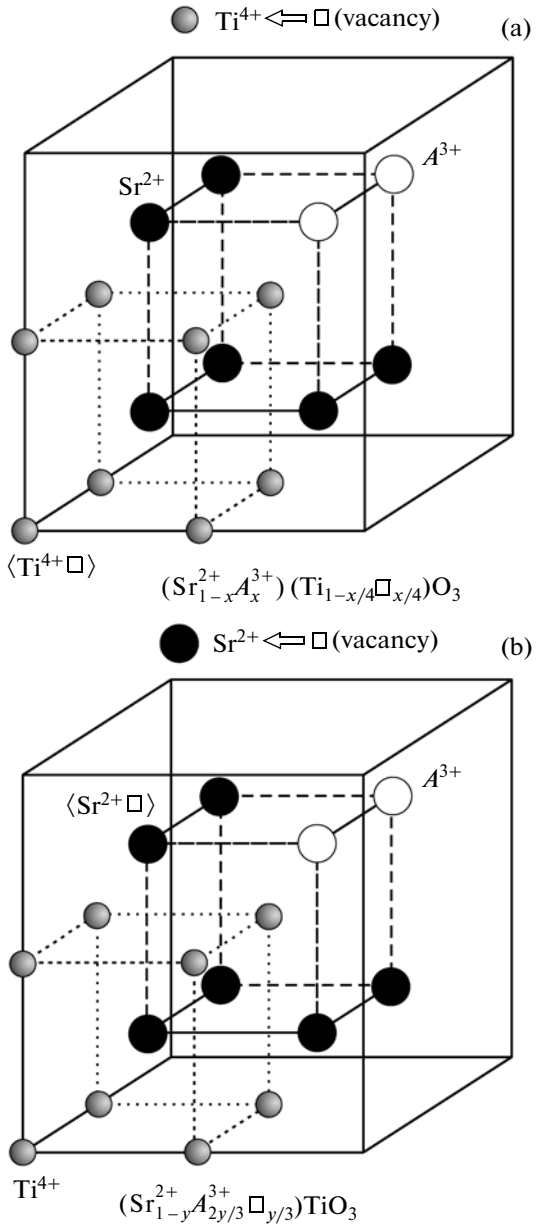

Fig. 1. Superlattice consisting of eight perovskite cells (2 × 2 × 2), containing 40 atoms (A^{3+} are the trivalent ions Sc^{3+}, In^{3+}, La^{3+}, and Bi^{3+}; □ is vacancy). Oxygen ions are not shown to simplify the figure. In the cases of (a) titanium and (b) strontium site vacancy formation, the "virtual" ion (⟨Ti□⟩, ⟨Sr□⟩) is at the corresponding site, where Ti(Sr) ions are mixed with the vacancy in the "virtual" crystal approximation.

orderings of heterovalent ions Sr^{2+} and impurities A^{3+}, and then the averaging over the entire set of lattices was performed. Due to the electrostatic interaction, configurations where impurity ions occupy neighboring positions will be most preferred. Therefore, as a supercell, we used a superlattice consisting of eight perovskite cells (2 × 2 × 2) and containing 40 atoms (Fig. 1).

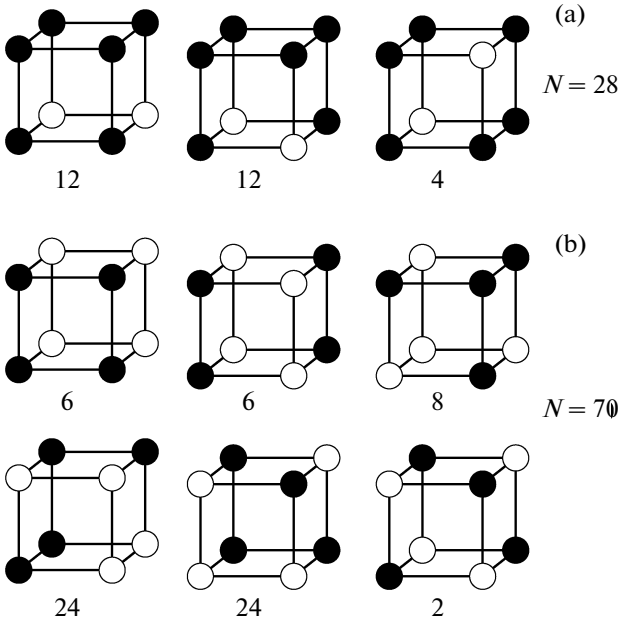

Fig. 2. Ordered structures with various energies for concentrations x = (a) 0.25 and (b) 0.50. Weight factors are given under the structures. N is the total number of the structures. Closed and open circles correspond to the strontium and trivalent impurity ions, respectively.

As noted above, when trivalent impurity ions occupy strontium sites, two ionic mechanisms of charge compensation are possible in the perovskite structure, i.e., the vacancy formation at the titanium or strontium site. In the former case, Ti^{4+} ions and vacancies were mixed at this site. In this case, we considered compositions with impurity concentrations $x = 0.25$ ($Sr_{0.75}A_{0.25}Ti_{0.9375}O_3$) and $x = 0.5$ ($Sr_{0.5}A_{0.5}Ti_{0.875}O_3$). In the case of strontium site vacancy formation, we considered only the case when two of eight Sr^{2+} ions in the superlattice are substituted with trivalent impurity ions. In this case, one vacancy is formed, which "is spread" over six remained strontium ions. Such an impurity concentration corresponds to the composition $(Sr_{0.833})_{0.75}A_{0.25}TiO_3$ ($y = 3/8$).

In the superlattice containing 40 atoms, for impurity concentrations $x = 0.25$ and 0.50, 28 and 70 various configurations of ordering trivalent ions are possible, respectively. However, not all these configurations have different energies. Figure 2 shows the configuration types with different energies and weight factors. For each of these structures, the dynamic matrix was calculated, vibration frequencies were calculated, and eigenvectors corresponding to soft ferroelectric modes were determined. Then, the dependence of the total energy of the doped crystal on the amplitude of ion displacements along eigenvectors of ferroelectric modes was calculated in each structure, and the energy was averaged over the entire set of superlattices. The same procedure was also performed to determine the

Table 1. Frequencies of ferroelectric modes (cm^{-1}) for various ordered structures and in the virtual crystal approximation (the mode degeneration is given in parentheses)

Structure	Sc^{3+}	In^{3+}	La^{3+}	Bi^{3+}
Titanium site vacancy, $x = 0.25$				
Structure 1	163*i*(2), 168*i*	73*i*(2), 54*i*	64*i*(2), 39*i*	67*i*(2), 37*i*
Structure 2	215*i*(2), 169*i*	131*i*(2), 75*i*	106*i*(2), 65*i*	108*i*(2), 66*i*
Structure 3	185*i*(3)	86*i*(3)	77*i*(3)	80*i*(3)
Virtual crystal	77*i*(3)	33*i*(3)	10*i*(3)	20*i*(3)
Titanium site vacancy, $x = 0.5$				
Structure 1	206*i*(2), 174*i*	98*i*(2), 75*i*	80*i*(2), 66*i*	82*i*(2), 66*i*
Structure 2	219*i*(3)	109*i*(3)	93*i*(3)	98*i*(3)
Structure 3	221*i*(2), 233*i*	101*i*(2), 106*i*	89*i*(2), 96*i*	90*i*(2), 94*i*
Structure 4	225*i*(2), 231*i*	118*i*(2), 124*i*	103*i*(2), 109*i*	107*i*(2), 112*i*
Structure 5	229*i*(2), 189*i*	125*i*(2), 82*i*	113*i*(2), 72*i*	117*i*(2), 68*i*
Structure 6	244*i*(3)	130*i*(3)	116*i*(3)	118*i*(3)
Virtual crystal	140*i*(3)	82*i*(3)	68*i*(3)	70*i*(3)
Strontium site vacancy, $x = 0.25$				
Structure 1	163*i*(2), 161*i*	79*i*(2), 51*i*	82*i*(2), 50*i*	80*i*(2), 42*i*
Structure 2	214*i*(2), 172*i*	126*i*(2), 88*i*	108*i*(2), 88*i*	113*i*(2), 84*i*
Structure 3	185*i*(3)	90*i*(3)	86*i*(3)	86*i*(3)
Virtual crystal	77*i*(3)	34*i*(3)	33*i*(3)	33*i*(3)

polarization vector **P**: for each structure, the polarization vector components

$$P_\alpha^n = U\sum_{k=1}^{N_{\text{atom}}}\sum_{\beta=1}^{3} Z_{\alpha\beta}^n(k)\xi_\beta^n(k),$$

were calculated, which were then averaged over all structures. Here the superscript n is the number of the ordered structure, $Z_{\alpha\beta}^n(k)$ are components of the matrix of the Born dynamic charge at the k-th ion, $\xi_\beta^n(k)$ is the eigenvector of the polar mode, and U is the amplitude of ion displacement along the eigenvector.

Here the following should be noted. In the compounds under consideration, as in many crystals with a perovskite structure, along with ferroelectric instability, the lattice vibration spectrum shows the unstable mode of the Brillouin zone boundary point, whose displacements along the eigenvector result in TiO_6 octahedron "rotation." In structures with a certain impurity position in the lattice, the soft vibrational mode corresponding to the octahedron "rotation" is absent, since, along with oxygen displacements, displacements of other ions appear in this mode. However, to solve the problem of the effect of antiferrodistortion ordering on ferroelectric instability in the ordered structures under consideration, we performed distortions corresponding to the TiO_6 octahedron "rotation."

All calculations were conducted at the experimental parameter of the $SrTiO_3$ perovskite cell ($a = 3.9$ Å).

3. RESULTS AND DISCUSSION

In the present calculation, pure $SrTiO_3$ has an unstable mode $\omega_R = -43$ cm^{-1} at the Brillouin zone boundary, whose eigenvector corresponds to the TiO_6 oxygen octahedron "rotation." The polar mode in pure $SrTiO_3$ is stable, although it has a low frequency $\omega_S = 17$ cm^{-1}. Table 1 lists the frequencies of soft ferroelectric modes, calculated for each structure type (Fig. 2); for comparison, the frequencies of these modes, calculated in the virtual crystal approximation are given.

As seen in Table 1, magnitudes of ferroelectric mode frequencies obtained in the virtual crystal approximation are significantly lower than the frequencies calculated in various ordered structures. Dynamic charges $\hat{Z}$ of ions and the high-frequency permittivity ε_∞ calculated for various structures slightly vary from structure to structure. Table 2 lists the dynamic charges and permittivities for one of the structures of each compound.

In the virtual crystal approximation, dynamic charges of titanium and oxygen are almost identical to the values given in Table 2. However, here the divalent strontium ion and trivalent impurity are mixed in the same position, and such a virtual ion has a dynamic

Table 2. Born dynamic charges and the high-frequency permittivity for some ordered structures in the "average" crystal approximation

Parameter	Sc^{3+}	In^{3+}	La^{3+}	Bi^{3+}
Titanium site vacancy, $x = 0.25$ (structure 3)				
ε_∞	5.43	5.45	5.57	5.68
$Z_{Sr,\,max}/Z_{Sr,\,min}$	2.70/2.53	2.70/2.55	2.71/2.64	2.71/2.71
Z_A	4.49	4.00	4.38	4.14
Z_{Ti}	5.74	5.75	5.77	5.8
$Z_{(),\,max}/Z_{(),\,min}$	−5.63/−1.60	−5.74/−1.50	−5.81/−1.53	−5.86/−1.5
Titanium site vacancy, $x = 0.50$ (structure 1)				
ε_∞	5.18	5.23	5.47	5.68
Z_{Sr}	2.35	2.39	2.57	2.71
Z_A	4.67	4.16	4.50	4.22
Z_{Ti}	5.13	5.15	5.20	5.24
$Z_{(),\,max}/Z_{(),\,min}$	−5.82/−1.95	−5.88/−1.73	−6.11/−1.81	−6.28/−1.74
Strontium site vacancy, $x = 0.25$ (structure 2)				
ε_∞	5.48	5.5	5.62	5.73
Z_{Sr}	2.2	2.2	2.2	2.2
Z_A	4.41	3.94	4.35	4.12
Z_{Ti}	6.36	6.37	6.4	6.42
$Z_{(),\,max}/Z_{(),\,min}$	−6.36/−1.15	−6.5/−1.15	−6.55/−1.15	−6.6/−1.15

Table 3. Displacements of Sr^{2+} and A^{3+} ions in the virtual crystal approximation and in the "average" crystal approximation (in relative units)

Impurity	Virtual crystal	"Average" crystal	Virtual crystal	"Average" crystal
Sc^{3+}	$\langle Sr_{0.75}Sc_{0.25}\rangle$	Sr 0.05	$\langle Sr_{5/6}Sc_{1/6}\rangle$	Sr 0.06
	0.27	Sr 0.55	0.26	Sc 0.53
In^{3+}	$\langle Sr_{0.75}In_{0.25}\rangle$	Sr 0.10	$\langle Sr_{5/6}In_{1/6}\rangle$	Sr 0.11
	0.27	In 0.45	0.25	In 0.42
La^{3+}	$\langle Sr_{0.75}La_{0.25}\rangle$	Sr 0.12	$\langle Sr_{5/6}La_{1/6}\rangle$	Sr 0.10
	0.25	La 0.42	0.24	La 0.39
Bi^{3+}	$\langle Sr_{0.75}Bi_{0.25}\rangle$	Sr 0.11	$\langle Sr_{5/6}Bi_{1/6}\rangle$	Sr 0.13
	0.26	Bi 0.40	0.24	Bi 0.36

charge of ≈3 for all compounds; meanwhile, we can see in Table 2 that the difference of the dynamic charge from the nominal one of impurity is larger than that of the Sr^{2+} ion.

The difference between the virtual and "average" crystal approximations is even more significant in the ferroelectric phase, in particular, in the study of the dependence of the doped crystal energy on the amplitude of ion displacement along the polar mode eigenvector, as shown as an example in Fig. 3a in the case of Sc^{3+} impurity at concentration $x = 0.25$. Table 3 lists the displacements of virtual ions $\langle Sr_{0.75}A_{0.25}\rangle$ ("titanium

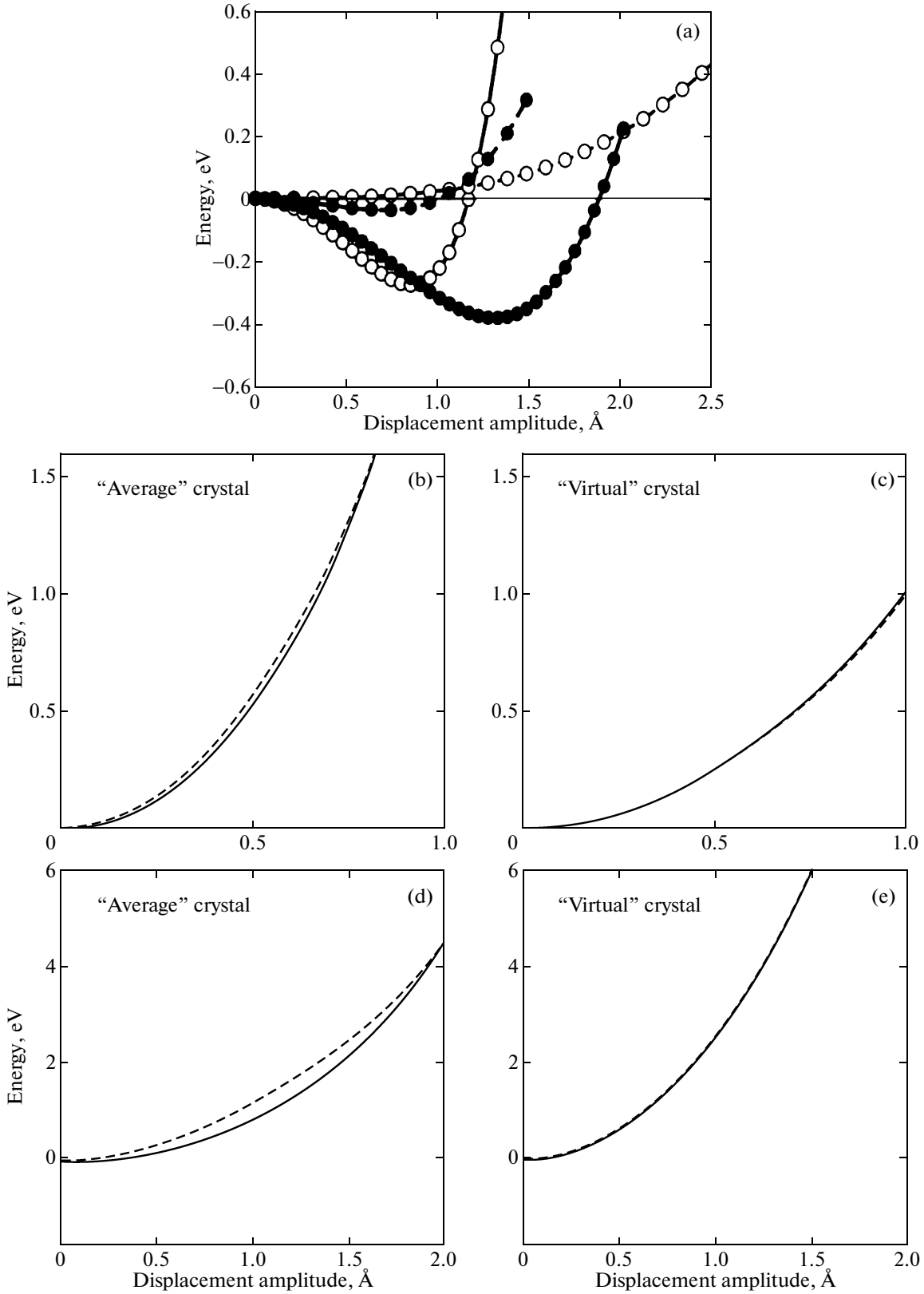

Fig. 3. Dependences of the energy on the ion displacement amplitude for $SrTiO_3$ doped with Sc^{3+} ions ($x = 0.25$). (a) Total energy (solid and dashed curves correspond to the "average" and "virtual" crystal approximations, respectively; closed and open circles correspond to the titanium and strontium site vacancies, respectively; (b), (c) sums of the dipole and Coulomb energies (solid curve) and the short-range energy (dashed curve) in the cases of titanium site vacancy formation for the "average" and "virtual" crystal approximations, respectively; and (d), (e) the same for the case of strontium site vacancy formation.

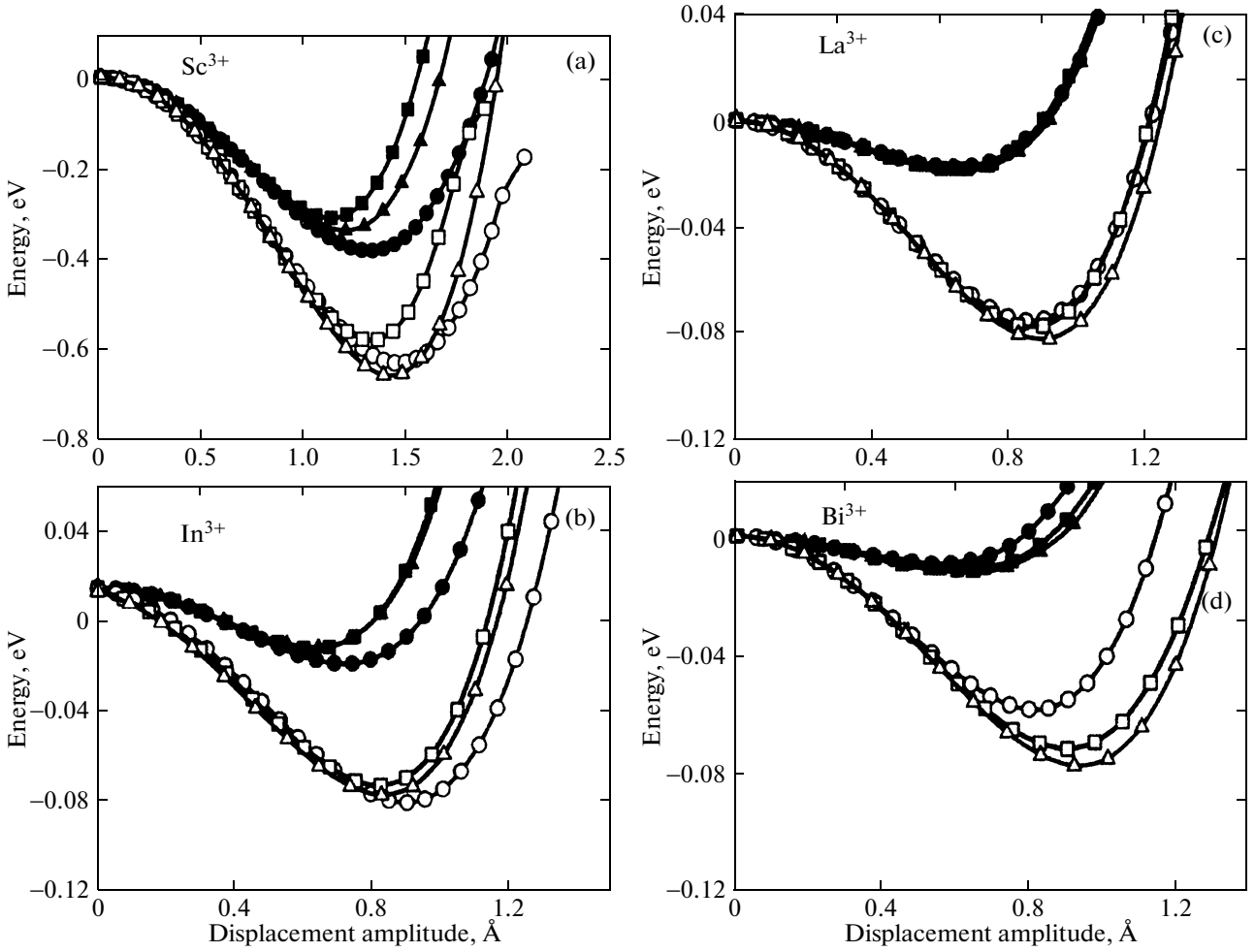

Fig. 4. Dependences of the total energy on the displacement amplitude for various types of trivalent impurities with concentrations $x = 0.25$ and 0.50 (closed and open symbols, respectively) for the [100], [110], and [111] crystallographic directions (circles, squares, and triangles, respectively): (a) Sc^{3+}, (b) In^{3+}, (c) La^{3+}, and (d) Bi^{3+}.

vacancy") and $\langle Sr_{0.625}\square_{0.125}A_{0.25}\rangle$ ("strontium vacancy") along the eigenvector of the ferroelectric mode and displacements of separated ions Sr^{2+} ($Sr^{1.67+}$) and A^{3+} averaged over all structures (Fig. 2). We can see that strontium ion displacements are negligible; major displacements are inherent to trivalent impurity ions.

This factor, along with larger dynamic charges of impurity, leads to a significant difference of the dependences of the long-range contributions to the doped crystal energy on the amplitude of ion displacement from the dependences in the case of the virtual crystal approximation, especially at large amplitudes. Figures 3b–3e shows the dependences of the short-range energy and the sum of Coulomb and dipole energy magnitudes on the amplitude of ion displacement. In the virtual crystal approximation in the case of titanium vacancy formation (Figs. 3b and 3c), the short-range positive energy is almost completely compensated by the negative Coulomb and dipole energies; whereas, there is no such compensation in the "average" crystal, which does cause deeper energy minima in the ferroelectric phase. In the case of strontium vacancy formation (Figs. 3d and 3e) in the "average" crystal, the difference between short-range and long-range energies is significantly smaller than in the

Table 4. Spontaneous polarization (C/m^2) in the "average" crystal approximation

Phase	Sc^{3+}	In^{3+}	La^{3+}	Bi^{3+}
Titanium site vacancy, $x = 0.25$				
Tetragonal	0.60	0.33	0.31	0.24
Orthorhombic	0.51	0.26	0.31	0.27
Rhombohedral	0.53	0.28	0.31	0.29
Titanium site vacancy, $x = 0.50$				
Tetragonal	0.64	0.31	0.40	0.33
Orthorhombic	0.58	0.29	0.42	0.37
Rhombohedral	0.60	0.29	0.46	0.38
Strontium site vacancy, $x = 0.25$				
Tetragonal	0.63	0.29	0.08	0.06
Orthorhombic	0.55	0.26	0.14	0.05
Rhombohedral	0.59	0.27	0.07	0.06

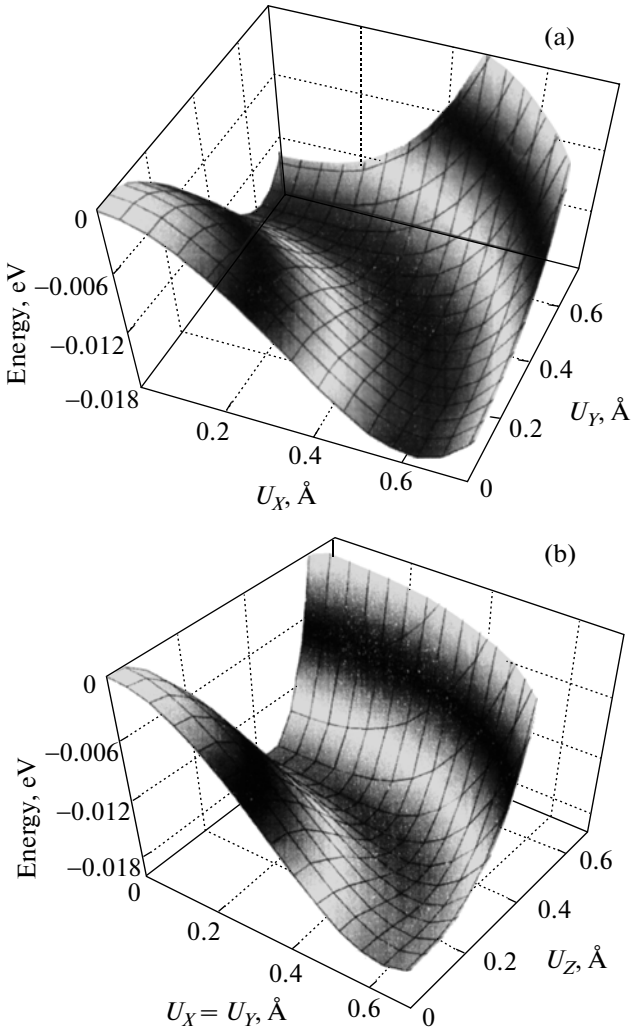

Fig. 5. Energy surfaces for $Sc_{0.75}La_{0.25}Ti_{0.9375}O_3$ (titanium site vacancy) with ferroelectric distortions; (a) combination of displacements along the [100] and [010] directions; and (b) combination of displacements along the [110] and [001] directions. U_X, U_Y, and U_Z are the amplitudes of ion displacements along the corresponding axes.

case of vacancies at titanium sites. However, in this case, the contribution of the short-range energy in the virtual crystal slightly exceeds the negative electrostatic energy, which results in the unfavorable ferroelectric phase in this approximation.

The maximum ion displacements in the ferroelectric phase were determined from the dependences of the total energy of the "average" crystal on the amplitude of these displacements along polar mode eigenvectors. Figure 4 shows these dependences for the case of titanium site vacancy formation for two impurity concentrations ($x = 0.25$ and 0.50). The energy minimum depth in the polar phase decreases with increasing impurity ion number in the Periodic table. The impurity type has also a significant effect on the polar phase symmetry in the ground state: in the case of doping with scandium and indium, the tetragonal phase with one polarization vector component (P_X, $P_Y = P_Z = 0$) is most favorable; in the case of doping with heavier lanthanum and bismuth, the rhombohedral phase with three equal polarization vector components ($P_X = P_Y = P_Z$) is most favorable. Table 4 lists the spontaneous polarizations averaged over all structures for all cases considered in this study.

Attention should be paid to the important result of this calculation. As seen in Fig. 4c, in the case of La^{3+} impurity for concentration $x = 0.25$ ($Sr_{0.75}La_{0.25}Ti_{0.9375}O_3$), the tetragonal, rhombohedral and orthorhombic ($P_X = P_Y$, $P_Z = 0$) phases have very close energies in a rather wide variation range of the amplitude of ion displacement. Figure 5 shows the energy surface for a combination of ion displacements along various directions. The energy surfaces in Fig. 5a were obtained for a combination of displacement amplitudes $\{U_X, U_Y\}$; in Fig. 5b, the energy surfaces are calculated for a combination of three displacements $\{U_X = U_Y, U_Z\}$. We can see that this surface contains a "valley" along which a change in the direction of the polarization vector with amplitude $U = \sqrt{U_X^2 + U_Y^2} \approx 0.63$ Å (Fig. 5a) and $U = \sqrt{U_X^2 + U_Y^2 + U_Z^2} \approx 0.65$ Å (Fig. 5b) almost does not change the energy. The presence of such a "valley" of minimum energy can lead to a situation when the spontaneous polarization vector freely rotates between three crystallographic directions. This situation is similar to the morphotropic phase boundary observed in (Pb, Zr)TiO_3 solid solutions [12]. Recently, the possibility of the existence of such frustrated polarization in the layered perovskite $PbSr_2Ti_2O_7$ was shown based on ab initio calculations [13]. For other impurity types, at the concentration $x = 0.25$, such a situation is not observed, since the energy of one of the phases is always lower than the energies two others (Fig. 4). For example, when adding In^{3+}, the rhombohedral and orthorhombic phases have very close energies, whereas the tetragonal phase is energetically more favorable.

Such a situation also does not arise as the impurity concentration increases. Figure 4 shows the dependences of the total energy of the "average" crystal on the amplitude of ion displacement along eigenvectors of the soft ferroelectric mode at $x = 0.5$ (titanium vacancy). In this case, for Sr^{3+}, La^{3+}, Bi^{3+} impurities, the rhombohedral phase is energetically more favorable; for In^{3+}, the tetragonal phase is such.

During the formation of vacancies at strontium sites, the energy minimum depth significantly decreases. Figure 6 shows the dependences of the total energy on the amplitude of ion displacement for the cases of titanium and strontium site vacancy formation at the impurity concentration $x = 0.25$. Such a decrease is probably associated mainly with an

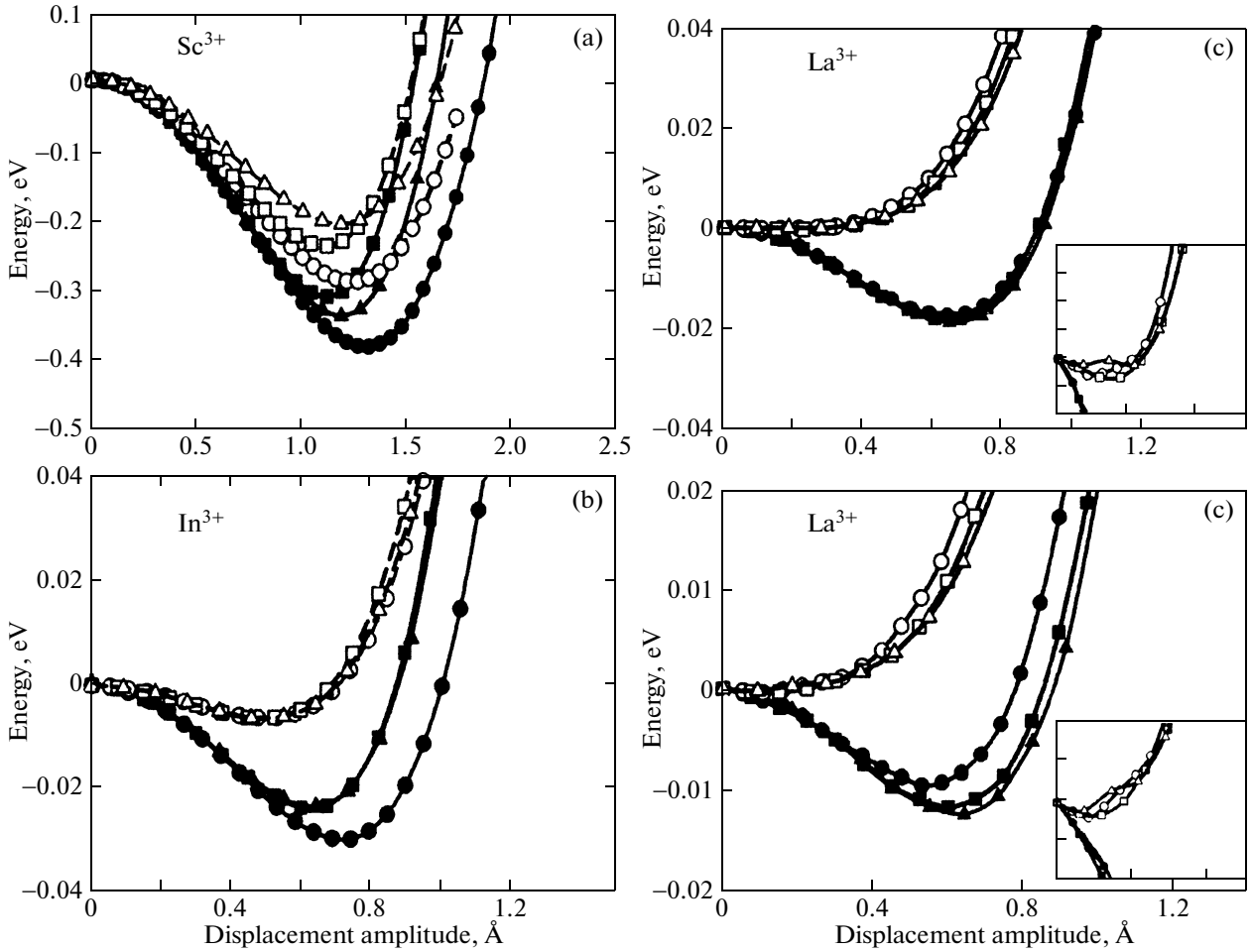

Fig. 6. Dependences of the total energy on the ion displacement amplitude ($x = 0.25$) for various types of trivalent impurities ((a) Sc^{3+}, (b) In^{3+}, (c) La^{3+}, and (d) Bi^{3+}) and various charge compensation mechanisms: titanium (closed symbols) and strontium (open symbols) site vacancy formation. Displacements along the [100], [110], and [111] (directions are indicated by circles, squares, and triangles, respectively). The insets (c) and (d) show these dependences for small displacement amplitudes.

increase in the contribution of the interaction of Ti^{4+}–O^{2-} ions to the short-range energy. In this case, the Coulomb attraction energy also increases; however, when ions approach each other along the eigenvector, the short-range positive energy increases more rapidly than the negative electrostatic energy decreases, as seen in Fig. 3d. In the present calculation, in the case of strontium vacancy, the ferroelectric state arises when strontium titanate is doped with scandium ions and is possible for doping with indium ions. Furthermore, when doping with indium, the situation of free rotation of the polarization vector is also possible. As seen in Fig. 6b, in the doped crystal $(Sr_{0.833})_{0.75}In_{0.25}TiO_3$, the energies of all three phases (tetragonal, orthorhombic, and rhombohedral) are close in a wide range of ion displacement amplitudes, and minimum-energy "valleys" are observed on energy surfaces (Fig. 7) at amplitudes $U = \sqrt{U_X^2 + U_Y^2} \approx 0.45$ Å and $U = \sqrt{U_X^2 + U_Y^2 + U_Z^2} \approx 0.48$ Å (spontaneous polarization $P \approx 0.27$ C/m^2). For La^{3+} and Bi^{3+} impurities, the ferroelectric transition is hardly probable.

As noted above, pure $SrTiO_3$ features antiferrodistortion instability. It is known [14] that antiferrodistortion distortions can lead to partial or total suppression of ferroelectric instability. To test this possibility, we calculated the dependences of the energy on the amplitudes of oxygen octahedron "rotation" in the "average" crystal approximation for all compounds under consideration. Such antiferrodistortion distortions appear energetically favorable in all compounds; however, the energy minimum depth associated with them is significantly smaller than the energy of ferroelectric distortions. As an example, this situation is illustrated for $Sr_{0.75}Sc_{0.25}Ti_{0.9375}O_3$ and $(Sr_{0.833})_{0.75}In_{0.25}TiO_3$ compounds in Fig. 8. It shows the dependence of the total energy of doped crystals on the displacement amplitude along the eigenvector of the ferroelectric mode in

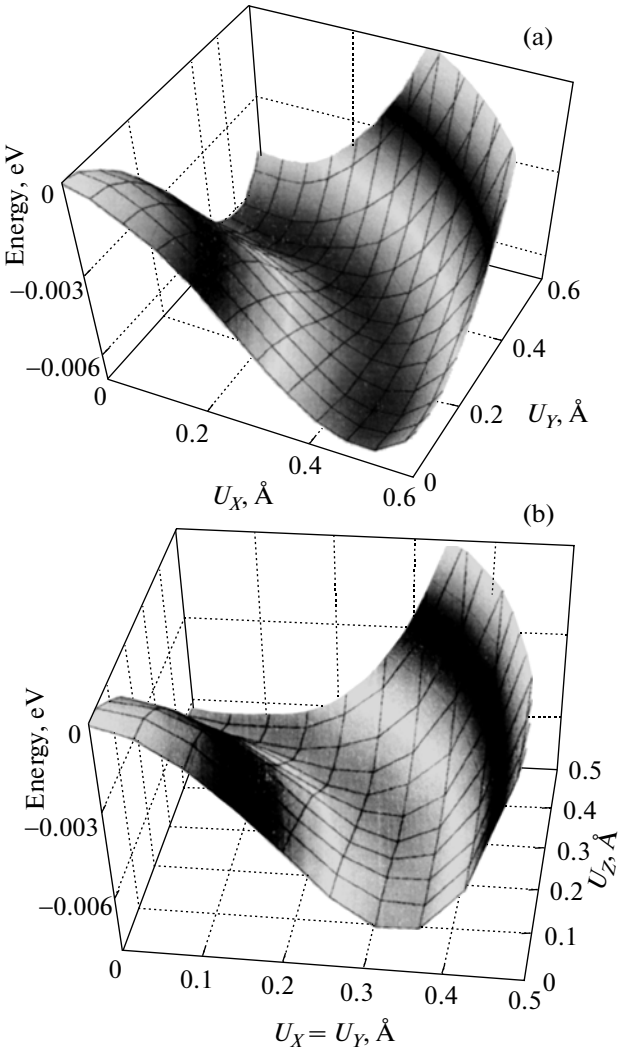

Fig. 7. Energy surfaces for $(Sr_{0.833})_{0.75}In_{0.25}TiO_3$ (strontium site vacancy) with ferroelectric distortions; (a) combination of displacements along the [100] and [010] directions; and (b) combination of displacements along the [110] and [001] directions. U_X, U_Y, and U_Z are the ion displacement amplitudes along the corresponding axes.

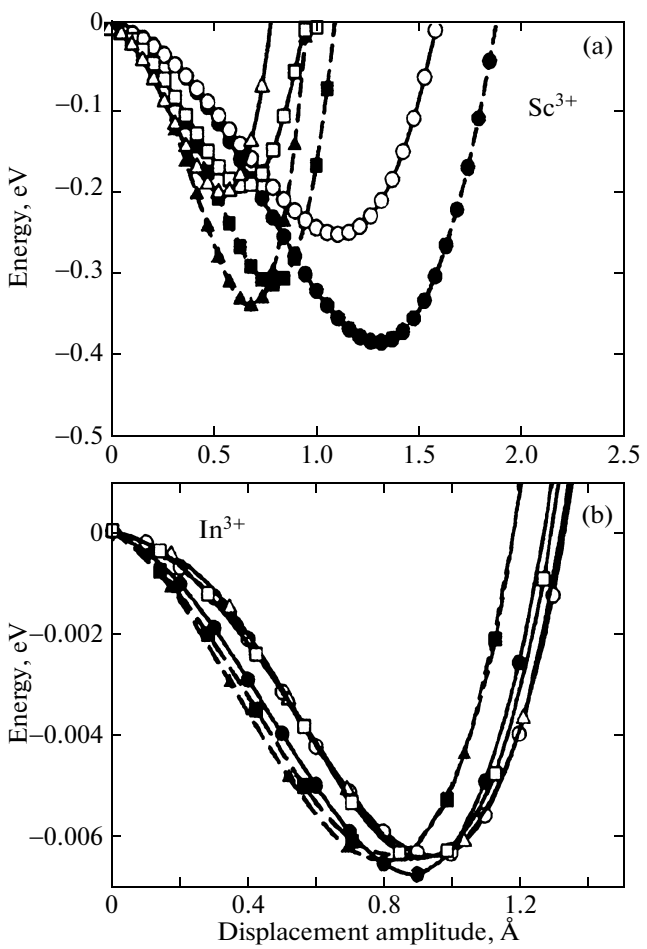

Fig. 8. Dependence of the total energy on the ion displacement amplitude in the case of ferroelectric distortions without (closed symbols) and with (open symbols) consideration of octahedron "rotation" in (a) $Sr_{0.75}Sc_{0.25}Ti_{0.9375}O_3$ and (b) $(Sr_{0.833})_{0.75}In_{0.25}TiO_3$. Distortions along the [100], [110], and [111] directions are shown by circles, squares, and triangles, respectively.

the phase where the oxygen octahedron was "rotated" by an angle corresponding to the energy minimum. The antiferrodistortion distortion has the strongest effect on compounds with scandium, where the energy minimum depth decreases more than by 30%. The effect of antiferrodistortion distortions on compositions with other impurity types is insignificant, as seen in Fig. 8 by the example of $(Sr_{0.833})_{0.75}In_{0.25}TiO_3$.

4. CONCLUSIONS

Within the generalized ionic crystal model, the lattice dynamics and ferroelectric instability in doped compounds $Sr_{1-x}A_xTi_{1-x/4}\square_{x/4}O_3$ and $Sr_{1-y}A_{2y/3}\square_{y/3}TiO_3$, where A is Sc^{3+}, In^{3+}, La^{3+}, and Bi^{3+}, were calculated. The ferroelectric instability was calculated using the approximation different from the virtual crystal approximation. In our opinion, the latter underestimates the Coulomb and dipole interactions in crystals doped with heterovalent impurity, which are especially important in studying ferroelectric distortions. Such an underestimation results in that the virtual crystal does not exhibit a ferroelectric state. The calculation showed that the ferroelectric phase is favorable in all the considered compositions. The energy minimum depth in the ferroelectric phase depends on both the impurity ion type and charge balance mechanism. The minimum is deeper when doping $SrTiO_3$ with light scandium ions; as the impurity ion number in the Periodic table increases, the energy minimum depth

decreases. The energy minimum depth in the polar phase also becomes smaller in the case of strontium site instead of titanium site vacancy formation. To a certain extent, this decrease is explained by the stronger attractive interaction of oxygen and titanium ions during strontium vacancy formation.

In our opinion, the most important result of calculations is the continuous minimum on the energy surface, obtained for some considered compounds: $SrTiO_3$ doped with La^{3+} ions, in the case of titanium site vacancy formation, and $SrTiO_3$ doped with In^{3+} ions in the case of strontium site vacancy formation at the concentration $x = 0.25$. The existence of such an energy minimum can lead to barrierless rotation of the polarization vector in the ferroelectric phase, which can be significant for applications of ferroelectric materials. However, it is very desirable to experimentally verify the result obtained.

In addition to ferroelectric instability, $SrTiO_3$ doped with trivalent ions exhibits instabilities associated with oxygen octahedron rotations. In all considered compounds, the effect of antiferrodistortion distortions on ferroelectric instability is negligible, except for compositions doped with Sc^{3+} ions.

ACKNOWLEDGMENTS

This study was supported by the Russian Foundation for Basic Research (project no. 09-02-00067), the Federal Program of Support for Leading Scientific Schools (project no. NSh-4645.2010.2).

REFERENCES

1. E. Dagotto, *Nanoscale Phase Separation and Colossal Magnetoresistance: The Physics of Manganites and Related Compounds* (Springer, Berlin, 2003).
2. *Colossal Magnetoresisitive Manganites*, Ed. by T. Chatterji (Kluwer, New York, 2004).
3. A. Kerfah, K. Taibi, A. Guehrai-Laidoudi, A. Simon, and J. Ravez, Solid State Sci. **8**, 613 (2006).
4. F. D. Morrison, D. C. Sinclair, and R. West, Int. J. Inorg. Mater. **3**, 1205 (2001).
5. A. Yamanaka, M. Kataoka, Y. Inaba, K. Inoue, B. Hehlen, and E. Curtens, Europhys. Left. **50**, 688 (2000).
6. V. V. Lemanov, E. P. Smirnova, E. A. Tarakanov, and P. P. Symikov, Phys. Rev. B: Condens. Matter **54**, 3151 (1996).
7. Chen Ang, Zhi Yu, P. M. Vilarinho, and J. L. Baptista, Phys. Rev. B: Condens. Matter **57**, 7403 (1998).
8. D. W. Johnson, L. E. Cross, and F. A. Hummel, J. Appl. Phys. **41**, 2828 (1970).
9. E. G. Maksimov, V. I. Zinenko, and N. G. Zamkova, Phys.—Usp. **47** (11), 1075 (2004).
10. L. Bellaiche and D. Vanderbilt, Phys. Rev. B: Condens. Matter **61**, 7877 (2000).
11. A. Mokhtari, J. Phys.: Condens. Matter **19**, 436213 (2007).
12. L. Bellaiche, A. Garcia, and D. Vanderbilt, Phys. Rev. B: Condens. Matter **64**, 060103-1 (2001).
13. S. M. Nakhmanson and I. Naumov, Phys. Rev. Lett. **104**, 097601-1 (2010).
14. S. M. Nakhmanson, Phys. Rev. B: Condens. Matter **78**, 064107 (2008).

Translated by A. Kazantsev